Thermochimica Acta, 100 (1986) 283–314
Elsevier Science Publishers B.V., Amsterdam – Printed in The Netherlands

THERMOANALYTICAL STUDY ON ANCIENT MATERIALS AND LIGHT IT SHEDS ON THE ORIGIN OF LETTERS AND WORDS

HANS G. WIEDEMANN
Mettler Instrumente AG, CH-8606 Greifensee/ZH (Switzerland)

G. BAYER
Institute of Crystallography and Petrography, ETH ZH, 8029 Zurich (Switzerland)
(Received 5 February 1986)

INTRODUCTION

Our knowledge about history today is quite comprehensive but certainly not complete. This is particularly true of the expressions of ancient peoples in terms of their languages. For example, the word "chemistry" is probably derived from the name of ancient Egypt "Kemet". This word actually means the "land of the black earth".

It was associated with the river Nile, which brought this black earth with it in the annual flood. Thus the name of the land of the black earth was created. Black earth leads to the word alchemy, magic chemistry; in German we use the expression "Schwarze Kunst". Actually, the whole life cycle in ancient Egypt was dependent on this black earth, brought by the river Nile more or less every year.

The real science of archeometry is rather young and goes back to the 18th Century. At that time Klaproth started to analyze ancient glasses. Since that time increasing numbers of chemists have been fascinated by the facts which chemical analysis can reveal about ancient history, ways of life, technical processes, products used and patterns of trade.

This paper is concerned with thermoanalytical methods, such as DSC, TG, TMA, analytical pyrolysis, X-ray diffraction and microscopy, which have been applied to the investigation of ancient materials.

The first example to be discussed concerns the trees of Queen Hatshepsut, which can be found on the temple walls in the Deir el Bahari and which are described in Egyptian history. The next chapter deals with our studies on Egyptian papyri. Some investigations follow on Egyptian glass and Nabataic pottery. New insight into the nature of ancient pigments is discussed afterwards. Finally, some thermoanalytical studies on Egyptian bronzes and Chinese silk are presented.

0040-6031/86/$03.50

TABLE 1

Family tree of Queen Hatshepsut

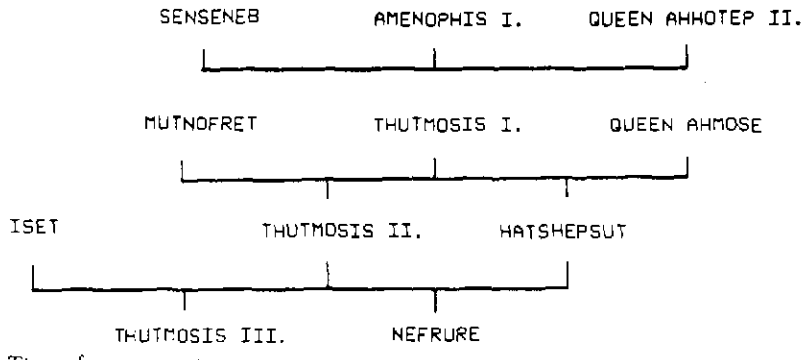

Time of government	
THUTMOSIS I.	1530–1520 B.C.
THUTMOSIS II.	1520–1505 B.C.
HATSHEPSUT	1505–1449 B.C.

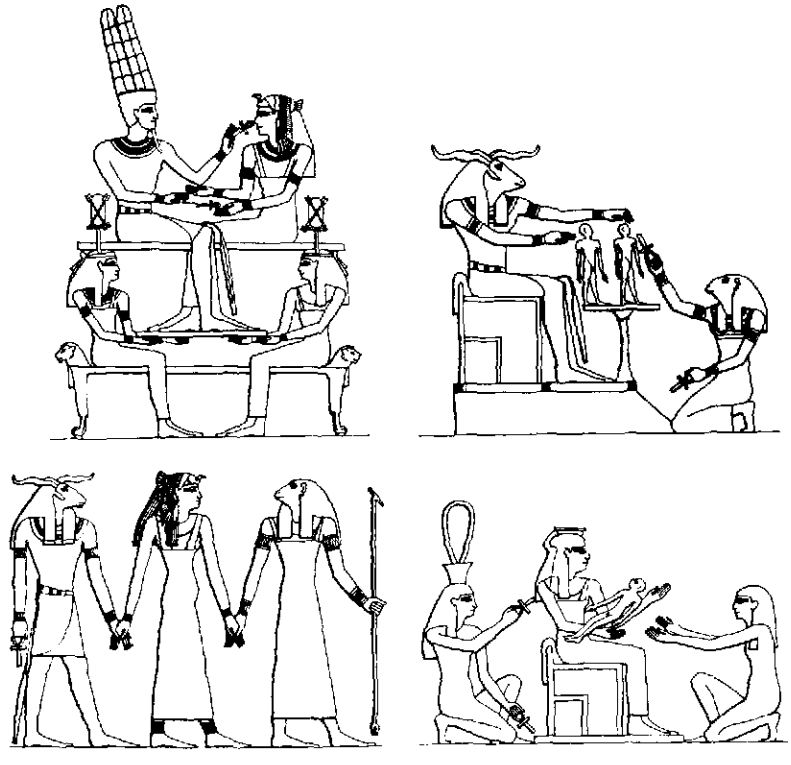

Fig. 1. Birth of Hatshepsut.

The experimental work was mainly carried out with the Mettler TA 3000 Thermosystem.

THE MYRRH TREES OF QUEEN HATSHEPSUT [1]

The birth of Hatshepsut, who was a pharaoh in the 18th Dynasty, was a special event in ancient Egyptian history. From the family tree shown in Table 1 one can see that Thutmosis I. and Ahmose were the parents of Hatshepsut. On the other hand the painted reliefs in the temple Deir el Bahari tell a different story (Fig. 1). According to these, god Amun visited Queen Ahmose, who afterwards gave birth to Hatshepsut by immaculate conception. Amun gave order to the god Chnum to form a child out of clay on the potter's wheel, which requires two figures, one representing the body, the other the soul. The mother—Queen Ahmose—is accompanied to the birth chair by two gods where she gives birth to Hatshepsut.

Instead of the expected son, a girl was born. This explains why Hatshepsut was regarded as male, up to the time where she became pharaoh. Only

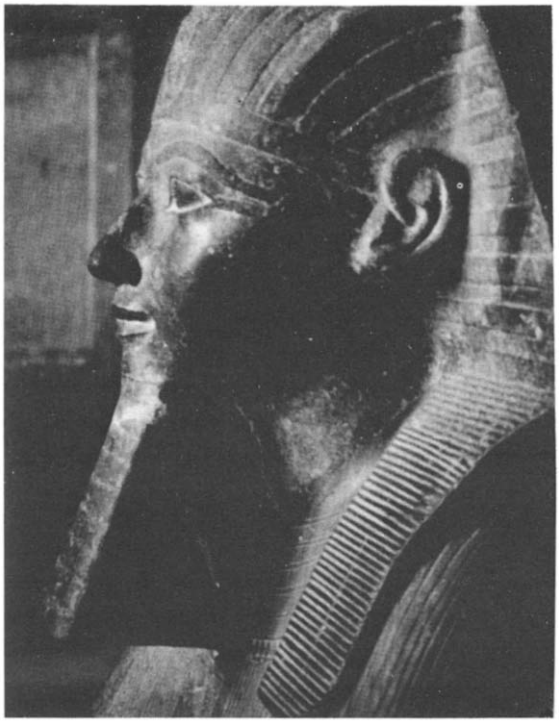

Fig. 2. Head of Queen Hatshepsut.

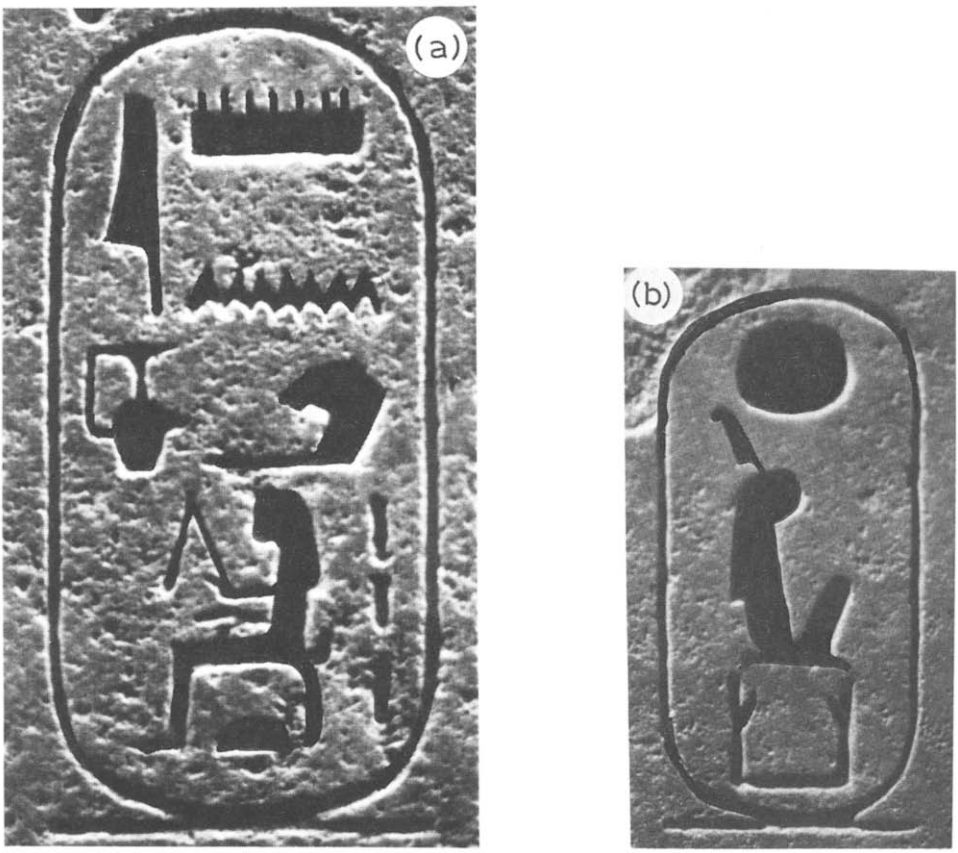

Fig. 3. Seals of Queen Hatshepsut.

during her regency was she officially considered and described as a female pharaoh. Perhaps another important event was that she was the first woman to be proclaimed as a pharaoh in ancient Egypt. She successfully ruled for more than 25 years and was a popular sovereign. According to the Old Testament she was also responsible for the education of Moses. However, this statement has not been proved historically.

Figure 2 shows the head of Queen Hatshepsut, which represents a part of a sphinx head. A further picture, Fig. 3, shows two of the seals of Queen Hatshepsut.

Hatshepsut built the temple of Deir el Bahari in Thebes to honor her father, the god Amun. This temple, which exists today and has been restored by Polish archaeologists, was the starting point of the present investigations.

The inscriptions which are still preserved on the temple walls tell of an expedition to Punt in Ethiopia. The purpose of this trip was to visit foreign countries in order to establish trade by bartering. Hatshepsut wanted to get some myrrh trees to decorate the temple of Amun. The pictures on the

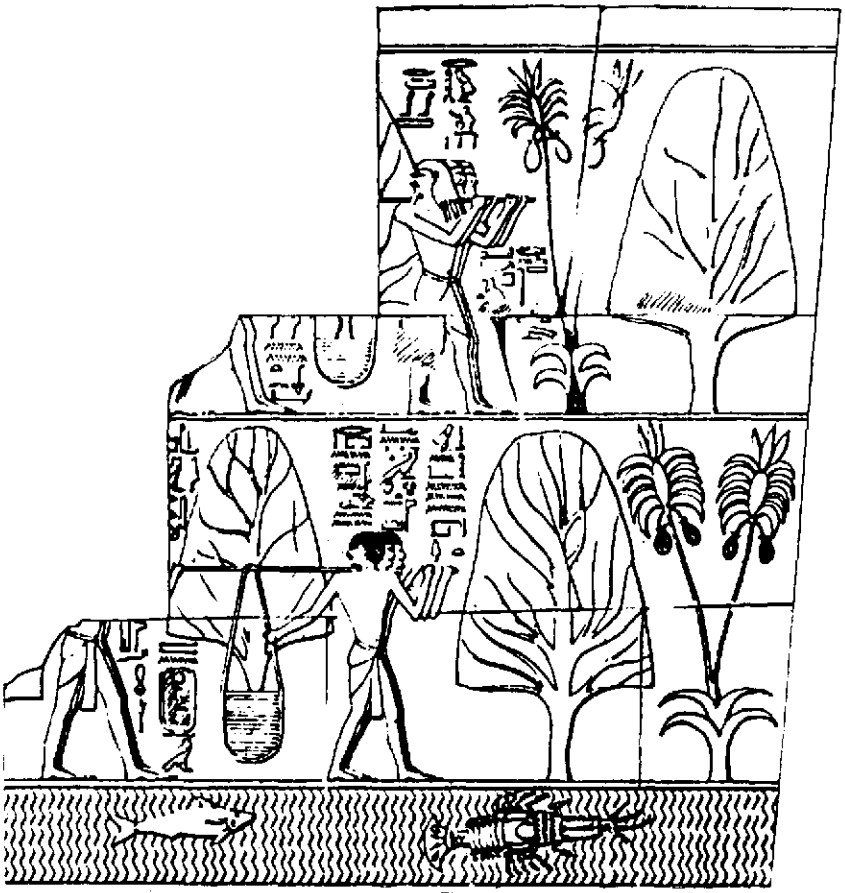

Fig. 4. Transport of the myrrh trees for transplanting (Deir el Bahari, Theben West, Egypt).

temple walls show the meeting of the ruling family, the presents which were made and also the transplanting of myrrh trees which had leather bags containing the humus on the roots (Fig. 4). Another picture shows the loading of the trees aboard the boats. Some of the stubs of these myrrh trees still exist in the temple area. It was possible to get a small amount of such material for investigations. The TG, DTG and DSC curves of these samples were recorded in oxidizing atmosphere (Fig. 5). They show different weight losses and degradation peaks of cellulose at 180°C and of lignin at 380–500°C. These results are similar to those obtained with papyri samples of the same period. This means that both the cellulose and the lignin contents have changed due to aging effects and by the surrounding sandy, dry soil. Isotope dating with C14 of the same tree stubs gave 2700 ± 110 years. The difference from the times of Hatshepsut may be due to the position from which the samples have been taken. In the case of the C14-method it was from the outside of a stub of 25 cm diameter. The growth

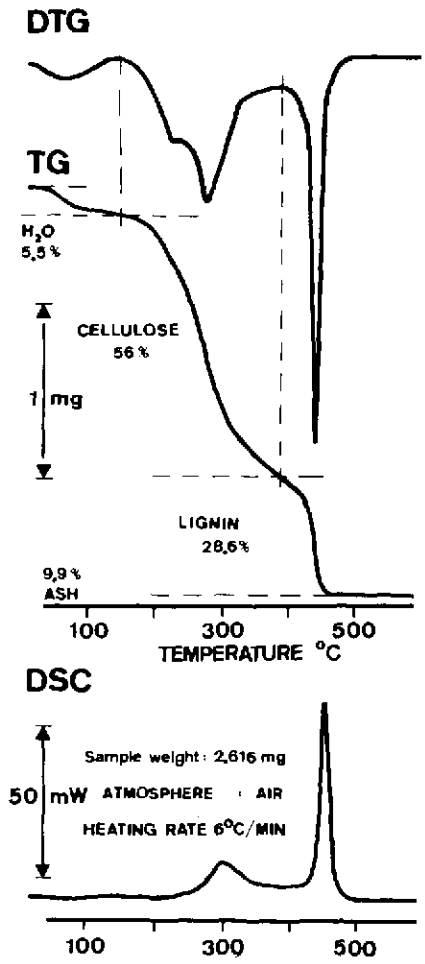

Fig. 5. TG, DTG and DSC curves of ancient tree stubs, the amounts of the various components are derived from the DTG curve by step analysis.

time of the trees in order to reach this diameter, however, is about 600 years.

Results of analytical pyrolysis with a linear mass spectrometer (Fig. 6) also proved that in the case of these myrrh tree stubs the dehydration process of cellulose goes from levoglucosan (mass 162) to levoglucosenon (mass 126), similar to that found for ancient papyri from the same era.

ANCIENT EGYPTIAN PAPYRUS [1b–5]

The actual writing material, papyrus, is made from the inner part of the stems after the bark has been stripped. Pictures of the 18th Dynasty, from the tomb of Puy-em-Re, show a man who is stripping the bark from a

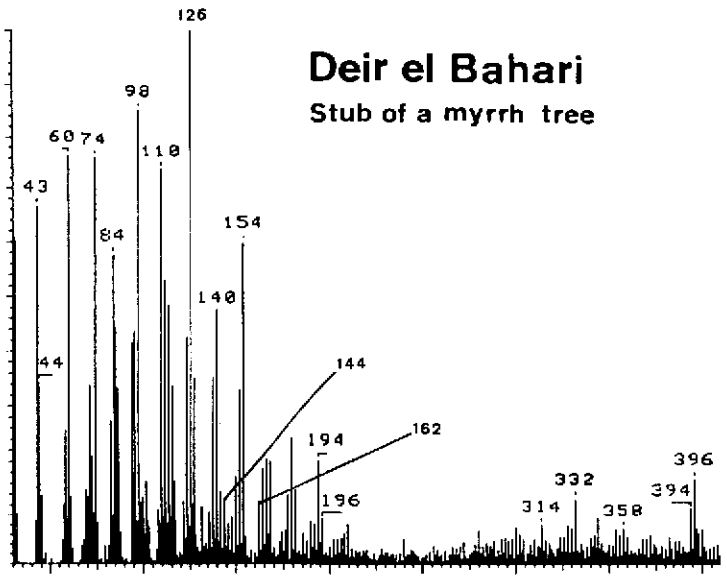

Fig. 6. MS curves of an ancient tree stub.

papyrus stem (Fig. 7a).

The DSC curves of different samples which were separated from a fresh papyrus stem are presented in Fig. 7b. The upper curve (a) is from a collateral bundle, which contains more "incrust" (lignin) than cellulose. The ratio of the cellulose peak (first peak) to the much stronger lignin peak (second peak) in the DSC curve is in accordance with this fact. The middle curve (b) corresponds to the cellulose region which surrounds the collateral bundle. It can be seen that cellulose and hemicellulose predominate whereas the lignin peak indicates the presence of monomeric and dimeric phenols in the form of a shoulder. The material of the third sample (curve c) was taken from the intermediate layer between the collateral bundle and the cellulose region. The DSC curve shows cellulose and hemicellulose to be more abundant than the monomeric phenols of lignin. The collateral bundle and the structure of a part of a papyrus stem in a thin section can be seen in Fig. 8. The position and the height of the lignin peak are particularly sensitive to the processing of the papyrus, to its age, and to its state of preservation.

To determine the differences in DSC curves caused by different treatments, we produced papyrus sheets using two different pretreatments: pressing and beating. Figure 9 shows the effect of the pretreatment on the shape of the peaks. The difference between the lignin peaks of the pressed papyri (curve a) and of the beaten papyri (curve b) is caused by mechanical destruction of the material, which results in a lowering of the heat of combustion. The small endothermic peak developed at 140°C (curve a) is caused by the dehydration of calcium oxalate monohydrate. To determine

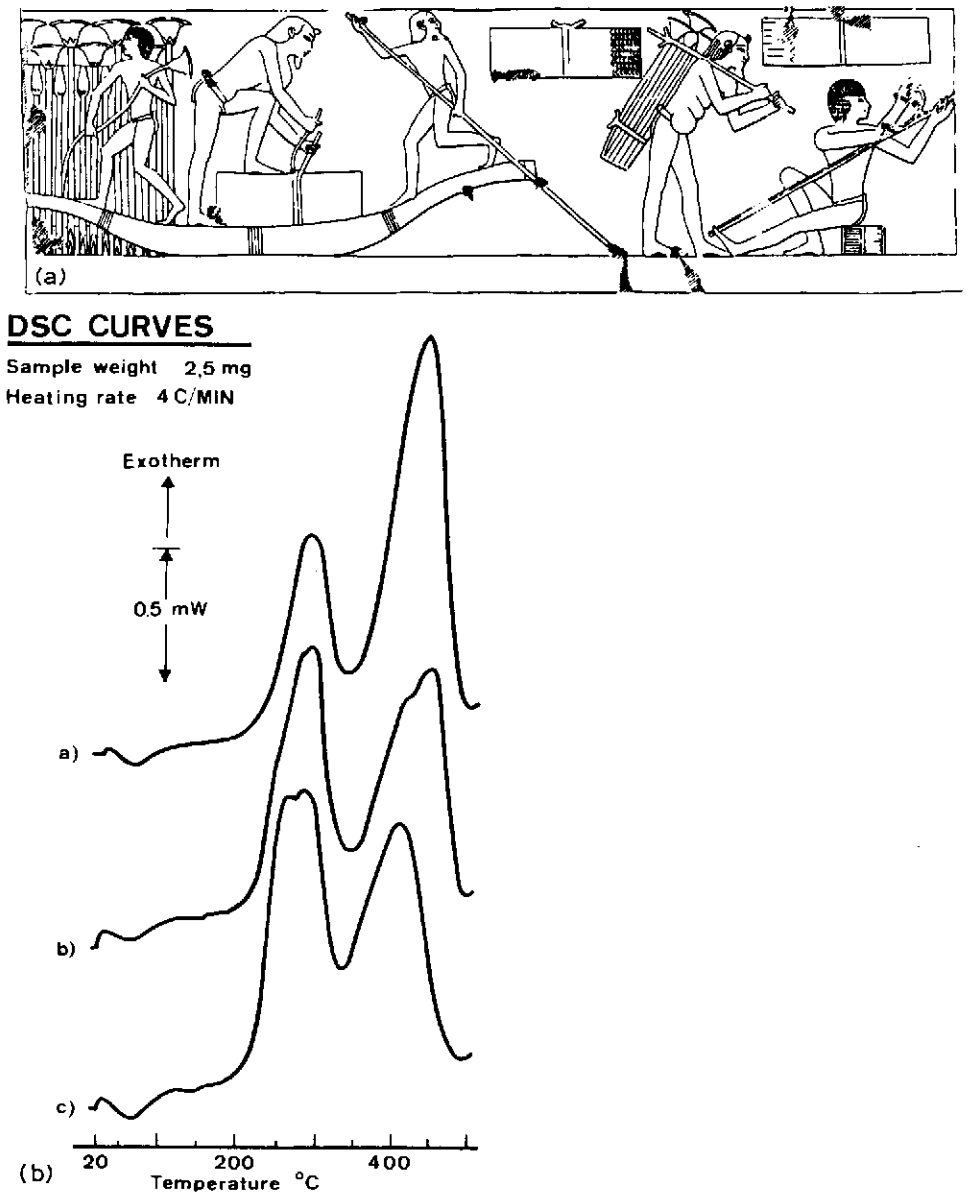

Fig. 7. (a) Harvesting, transport, and bark stripping of papyrus in ancient Egypt (Tomb Puy-em-Re, Theben West, Egypt). (b) DSC curves of the different regions of a papyrus stem.

how the lignin peak changes with age, we asked the Egyptian Museum in Berlin for dated samples from 600 B.C. to 600 A.D. DSC curves of these samples are shown in Fig. 10. These curves prove that the lignin peak decreases slightly with increasing age of the sample.

The swelling behavior of papyri was also investigated in relation to age by subjecting a number of papyri to dynamic TMA. Figure 11a shows the TMA

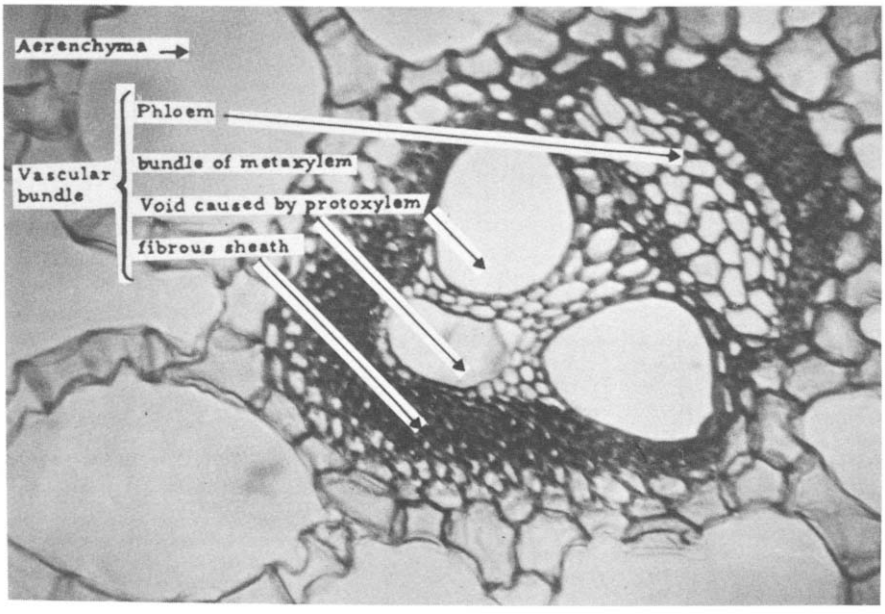

Fig. 8. Thin section of a part of a papyrus stem.

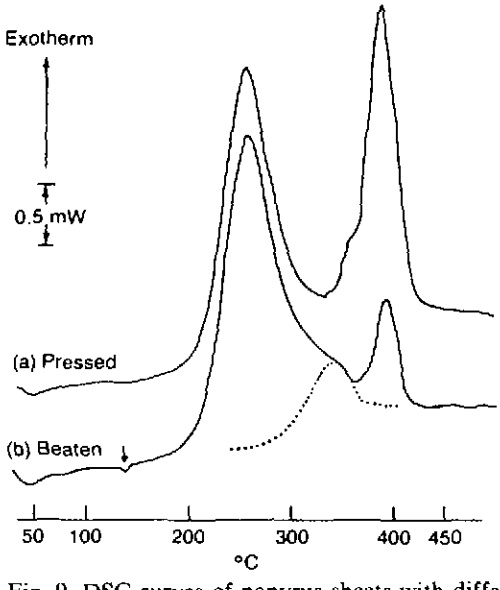

Fig. 9. DSC curves of papyrus sheets with different treatments.

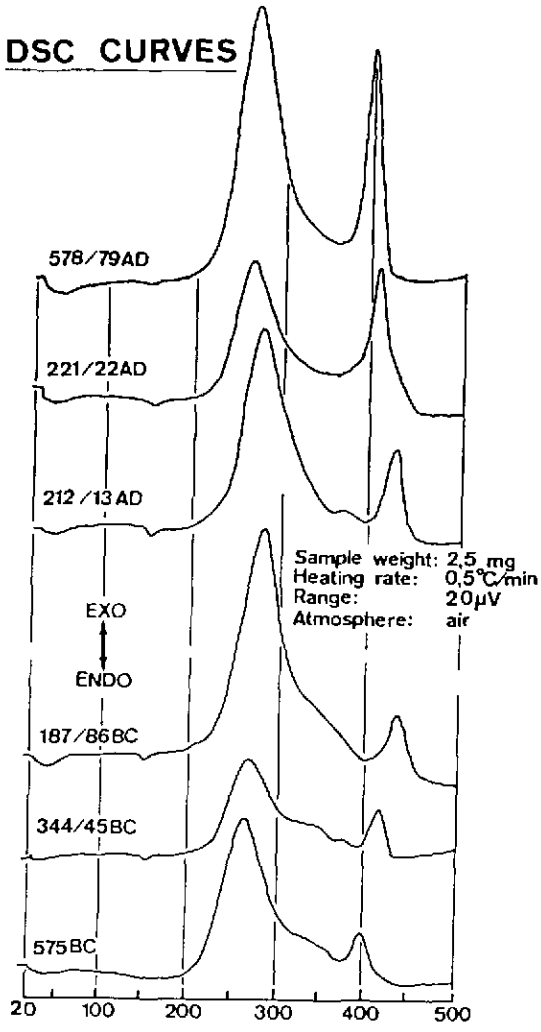

Fig. 10. DSC curves of various ancient papyri.

cell. The sample is placed between the vitreous silica platform and movable SiO_2 rod and subjected to a variable load. After equilibration for 3–5 min, water is added to the dish. Figure 11b shows the swelling behavior of a fresh and of an ancient papyrus sample. First there is a sudden contraction due to the imbibition with water, followed by parabolic swelling curve. Taking the fresh papyrus as a reference (100%), the ancient papyrus (578 A.D.) shows swelling of the order of 5–6%. Further experiments with ancient papyri from different periods showed that papyri from about 1000 B.C. swell by about 2–3% whereas papyri older than 1500 B.C. show no expansion at all. MS results of analytical pyrolysis on dated ancient papyri show that with

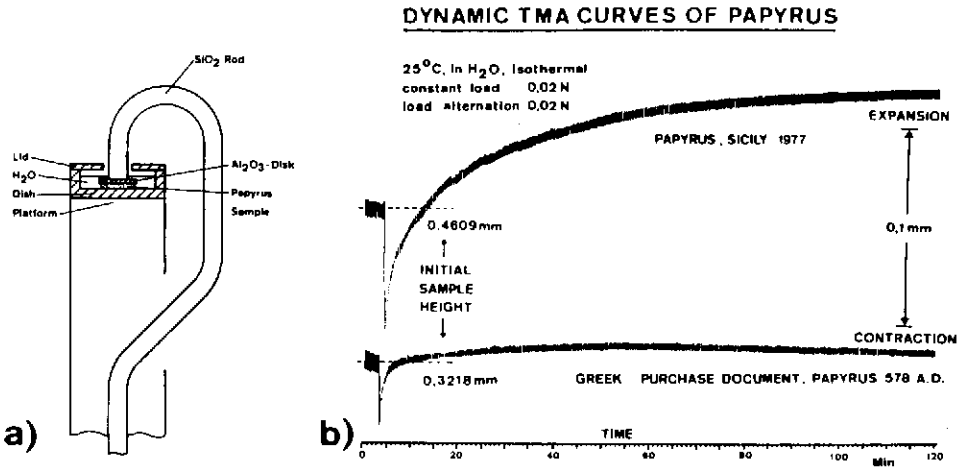

Fig. 11. (a) TMA cell and (b) TMA curves of fresh and ancient papyri.

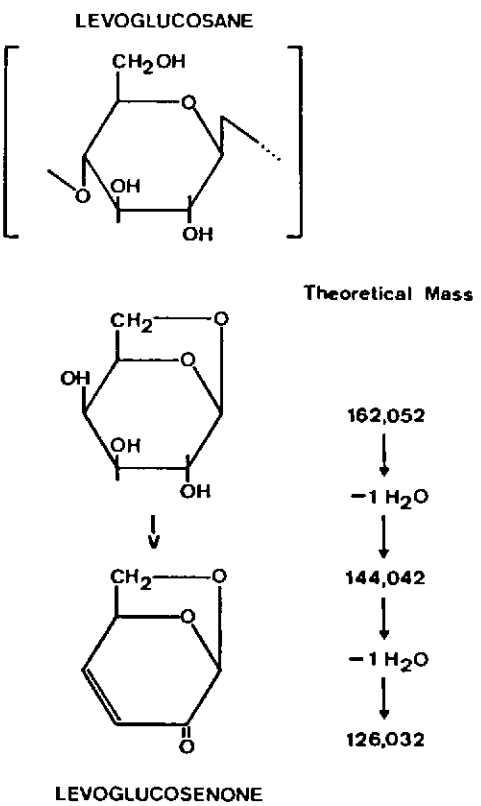

Fig. 12. Dehydration of cellulose by aging.

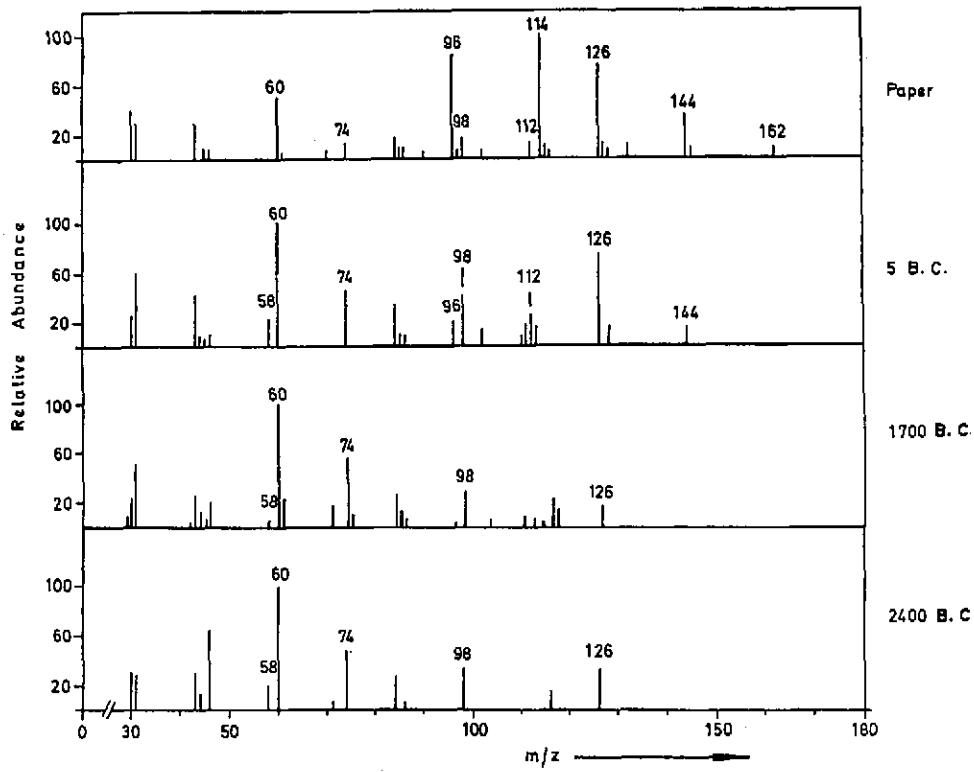

Fig. 13. MS curves of paper compared to papyri of different age.

increasing age the levoglucosan (162) becomes dehydrated to levoglucosenon (126). These results are shown in Figs. 12 and 13.

GLASSLIKE MATERIALS IN THE ANCIENT ORIENT [1b,6]

The beginning of glass production in ancient times is usually dated back to the 16th Century B.C., when the first hollow glassware appeared in Egypt. From the 4th millennium amorphous glazes on silica-based ceramics were already known in Egypt and Mesopotamia, and also some crystalline silicates.

The coloring of glasses was well developed in ancient Egypt. The usual colors were blue, yellow, white and red, which were obtained by addition to the glass of copper, cobalt and iron oxides for blue, lead antimonate for yellow, tin oxide for white and cuprous oxide for red. At about the same time as in Egypt similar glasses were produced in Mesopotamia, where the first written recipes for the production of glasses have been found. The cuneiform writings from the library of the Assyrian king Assurbanipal (669–629 B.C.) contain texts which give details about the mixing ratio of the

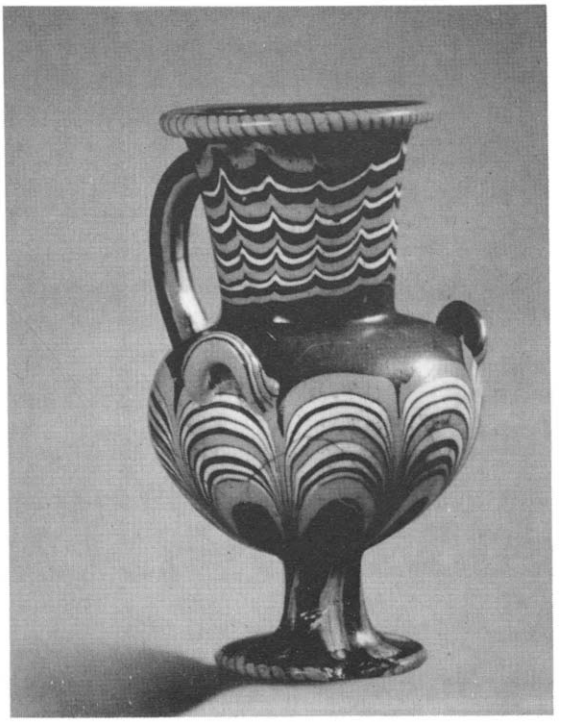

Fig. 14. Decorated glass vase from the Amarna period (1350/60 B.C.).

raw materials, the procedure of melting and the forming and checking of the glass objects. This information is in agreement with the findings of glass objects from ancient Egypt.

For the present investigations original samples of ancient Egyptian glass of the Amarna period (1350 B.C.) were used. Figure 14 shows a typically decorated glass vase from this period. A fragment of such a glass object was investigated. It is obvious that the yellow glassy stripes are inlaid in the blue

TABLE 2

Composition (%) of modern flat glass and of ancient glass (Amarna period)

	Ancient glass	Modern flat glass
SiO_2	60–70	69–73
Na_2O	15–25	12–16
CaO	4–10	8–10
MgO	1–5	2–4
Al_2O_3	0.5–3	1–2
K_2O	0.5–3	
Fe_2O_3	0.5–3	

TMA CURVE

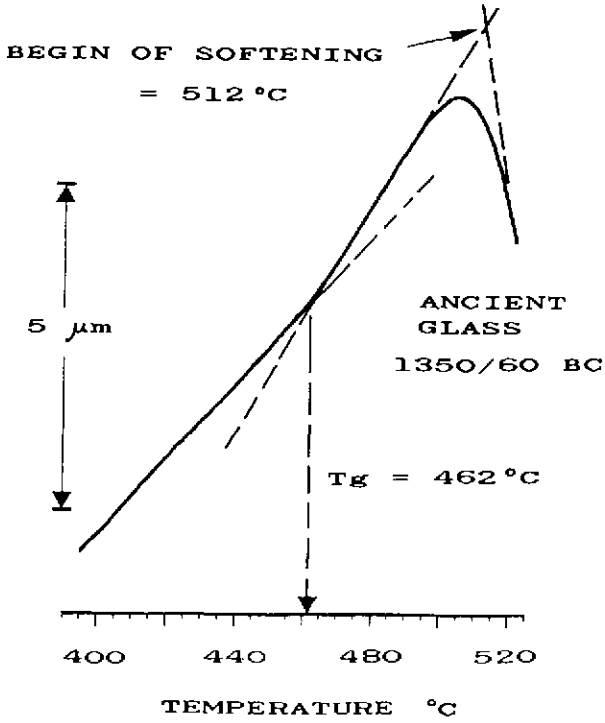

Fig. 15. TMA curve of ancient glass from the Amarna period, sample length 4.45 mm, heating rate 10°C min^{-1}.

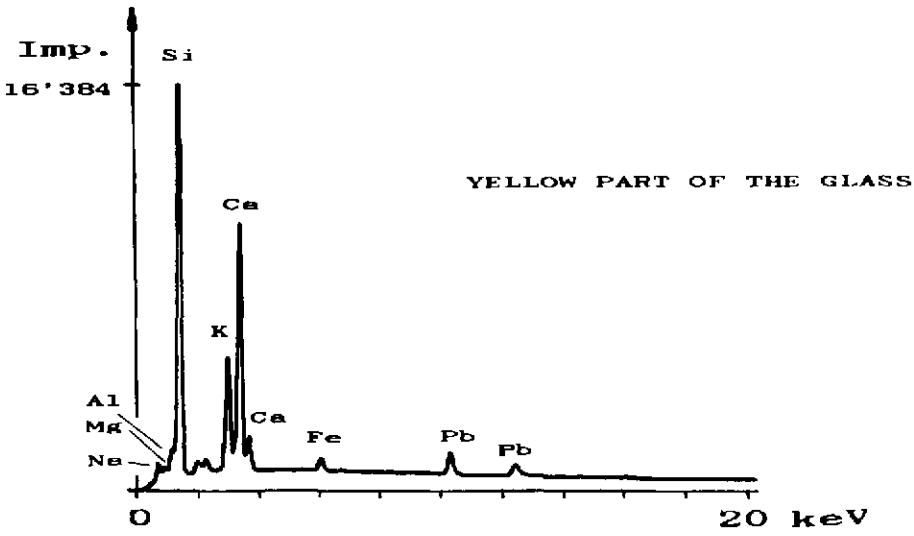

Fig. 16. EDAX analysis of the yellow region of glass, Amarna period.

base glass. The blue glass, which was slightly opacified by devitrification, showed the presence of a minor amount of crystalline phase of sodium calcium silicate. Figure 15 shows the expansion and softening behavior of the ancient blue glass measured by TMA. The position of the transformation point and the onset of softening can be derived from the TMA curves. These values are in the expected range of temperature and are found at lower temperatures for the ancient glass as compared to modern glass due to its higher alkali concentration. Table 2 compares the compositions of modern flat glass with ancient glass. Figure 16 refers to the EDAX analysis of the yellow part of the glass fragment. EDAX and X-ray analysis proved that the yellow color is probably caused by lead antimonate.

NABATEAN POTTERY [7,8]

Originally the Nabateans were Arabic beduines who lived in the desert of Hejas from the 6th to the 4th Century B.C. Later on they moved to the area of the Edomiter, today Jordan, and formed the township Petra. Petra means rock-like. In this period, many of the famous rock tombs were created around Petra and Hegra. The inlet of Petra from Wadi Mussa goes through a rock canyon which is called Bab es-Sik.

The Nabateans had their own language and script. It is interesting that if one puts the corresponding Nabataic expression between the modern Hebraic and Arabic words, one can see a definite relationship between them. Table 3 shows some examples of similarity in writing.

The typically painted Nabataic ceramics were manufactured between the first century B.C. and A.D. A variety of fragments of these thin-walled ceramics was studied with respect to the phase composition and to the thermal behavior. Two of these samples with quite different chemical composition, shown in Table 4, will be briefly discussed. The Fe_2O_3-rich and CaO-poor sample 25 in thin section shows only quartz as crystalline phase. The typical red-brown color of this ceramic is due to the use of iron-rich clays for its manufacture. Heating this sample for 1 h at 1000°C did not cause any changes of the X-ray pattern or color. After heating at 1100°C, crystallization of mullite and cristobalite was observed with a decrease of the quartz content. The DSC, TG and TMA analyses of this sample, shown in Fig. 17, proved that exothermic reactions with weight loss from carbonaceous residues occur at around 300 and 500°C, followed by the endothermic quartz transformation at 573°C. Strong sintering with corresponding deformation (see TMA curve) starts above 900°C. A completely different behavior was found for sample 26, which has high concentrations of CaO and MgO, but much less SiO_2 and especially Fe_2O_3 in comparison to sample 25. The X-ray pattern shows the presence of the following crystalline phase: quartz, augite (pyroxene), plagioclase and gehlenite. Again there was no

TABLE 3

Similarities in Hebraic, Nabataic and Arabic writings

Hebraic	Nabataic	Arabic
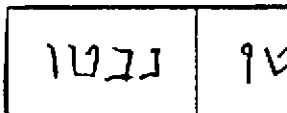	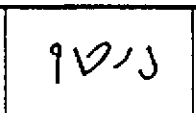	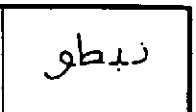
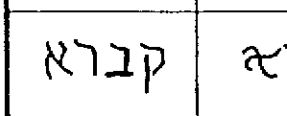	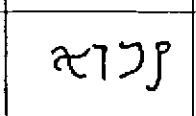	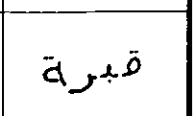
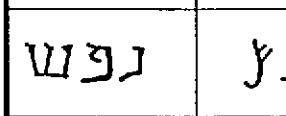	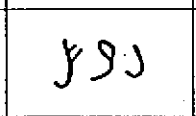	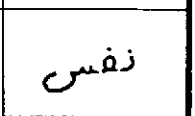
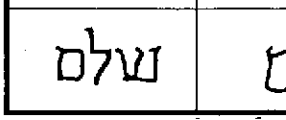	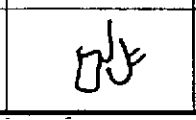	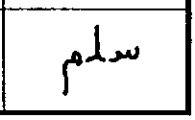

Examples of similarity in writing

Common root	Hebraic	Nabataic	Arabic	Meaning
N-B-Th-U	nabatu	nabatu	nabat	sprout
Q-V-R	qever	qevar	qabr	tomb
N-F-Sh	nefesh	nefash	nafs	soul
Sh-L-M	shaloin	shelam	salam	peace

change in phase composition after heating at 1000°C. Heating this cream-colored, strong ceramic material at 1100°C caused the disappearance of gehlenite and a strong increase of the plagioclase concentration, whereas the

TABLE 4

Chemical composition of Nabataic pottery (%)

Sample No:	25	26	Sample No:	25	26
Loss on ignition	1.77	2.86			
SiO_2	61.18	49.99	CaO	0.36	17.63
Al_2O_3	22.30	20.95	MgO	0.83	3.07
Fe_2O_3	8.50	1.80	K_2O	2.89	2.17
TiO_2	1.46	0.71	Na_2O	0.74	0.58
			Total	100.03	99.76

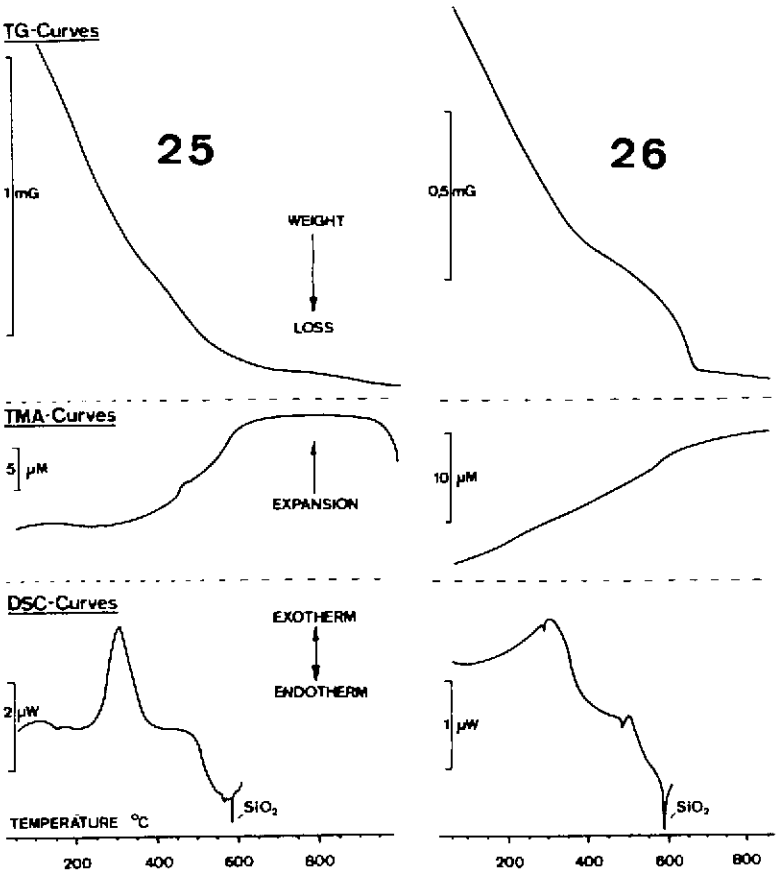

Fig. 17. TG, DSC and TMA curves of Nabataic pottery.

pyroxene phase did not change significantly. Formation of mullite could not be observed. The DSC and TG curves (Fig. 17) are somehow similar to those of sample 25, but the TMA curve proves that this ceramic does not show any shrinkage due to secondary sintering up to at least 1000°C. These preliminary results suggested that a $CaCO_3$-rich clay was used in the manufacture of this material and that the firing temperature was higher than for the other material but probably not much above 1000°C.

ANCIENT EGYPTIAN PIGMENTS [6,8–11]

Many of such colored materials were produced from natural minerals. However, a wide range of synthetic pigments was also used, mostly in the form of glass frits. This is especially true for the blue pigments which were much in demand, since blue was the color of the gods.

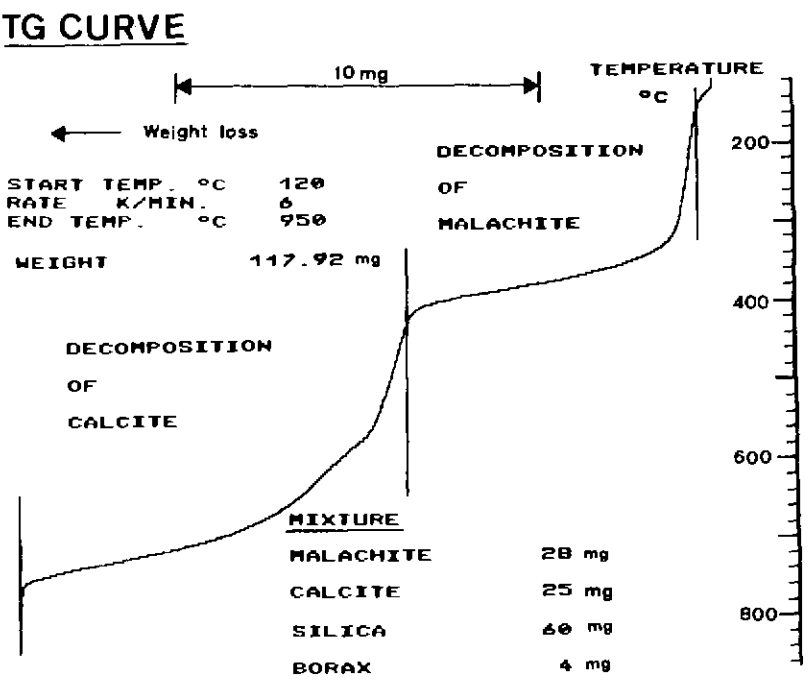

Fig. 18. TG of the formation of Egyptian Blue from the raw materials.

We had the unique possibility of investigating the blue pigment used to decorate the bust of Nefertiti. These studies proved that the blue pigment of the bust is indeed the crystalline compound $CaCu(Si_4O_{10})$—Egyptian Blue —and not a blue glassy frit as assumed by Rathgen. In further investigations we also found more detailed information about the experimental conditions for synthesis of this important blue pigment and its thermal stability. Egyptian Blue was already in use during the 4th Dynasty in Egypt, at about 2600 B.C., and was produced in consistent quality for more than 2000 years. For the thermal synthesis of Egyptian Blue we used calcite of the Cheops pyramid, azurite or malachite from Egyptian localities and sand from the desert as raw materials.

Four different fluxes were added to the above stoichiometric mixtures, namely borax, papyrus ash, salt or sodium sulfate. Figure 18 shows the thermogravimetric analysis of the formation of $CaCu(Si_4O_{10})$ from the mixture limestone/malachite/sand/borax as an example. The TG curve proves that the decomposition of malachite to CuO occurs at 300–400°C, followed by the decomposition of limestone to CaO at 550–740°C. Above this temperature CaO and CuO react with SiO_2 in the presence of the flux to form the compound $CaCu(Si_4O_{10})$. Figure 19 shows photometer curves of X-ray patterns of this synthetic Egyptian Blue product and of the original blue pigment taken from the bust of Nefertiti. The correlation is obvious.

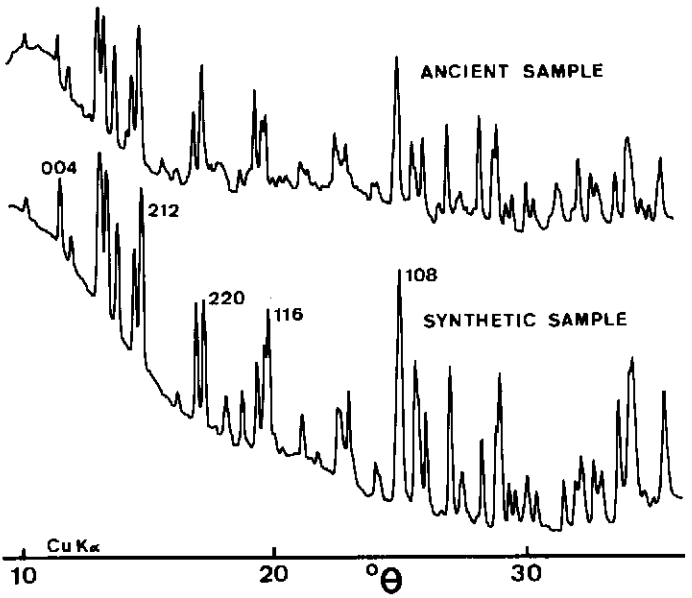

Fig. 19. X-ray photometer curves of synthetic and ancient Egyptian Blue.

The solid state reaction between azurite, calcium carbonate and sand also leads to the formation of Egyptian Blue and was studied by means of DSC. Quartz is the least reactive component in this mixture, therefore the decrease

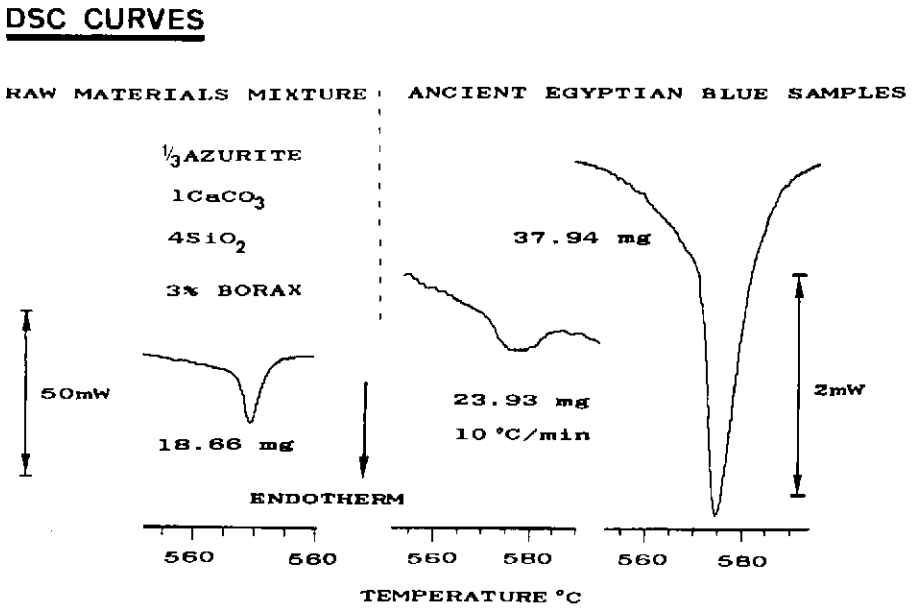

Fig. 20. DSC curves of the raw materials and of ancient Egyptian Blue samples.

of the quartz peak may be used as a criterion for the completeness of this reaction. These DSC results obtained on various ancient and synthetic Egyptian Blue samples also showed agreement with the intensity of the quartz reflections in the X-ray patterns of such samples. Very few of the ancient Egyptian Blue materials were completely free of unreacted quartz, for example those from the 18th Dynasty. Most of them contained varying amounts of unreacted quartz in spite of their bright blue color. As an example, the DSC curves of two such samples are shown in comparison with the raw material mixture which contained 53% quartz (Fig. 20). The ancient Egyptians were able to control this solid state reaction very well. The ancient name of this pigment is "hesbed". To differentiate synthetic blue and natural blue, for example lapizlazuli, a determinative is added to the word. In other words, if the expression "truth" appears at the end of the word hesbed, we have a natural sample. If the expression "crucible" appears, we have a synthetic sample.

EGYPTIAN BRONZES [1b,6]

The melting and use of bronzes in ancient Egypt is well documented. At the end of the 6th Dynasty, around 2500 B.C., the expression "asiatic copper" appeared. A relief in the tomb of Mereruka (6th Dynasty, Saqquara) shows the melting of bronze by workers with blowpipes. The liquid metal is then cast in bars or into a container, cooled down and formed into sheet metal. The weight of the cast bars is usually recorded in written form by a scribe (on the left-hand side). The expression "asiatic copper", with a slightly different spelling, was used for bronze in the 18th Dynasty, which was molten with tin.

Figure 21a shows Egyptian workers stepping on bellows with their feet (Tomb of Rehmire). The air is sucked in by lifting the bellows via cords with the hands. The crucibles are removed from the fire with two long flexible sticks and at the right-hand side in the picture the metal is obviously poured in forms. These two pictured scenes (on the Tombs of Mereruka and Rehmire) are separated by a period of about 1200 years. During this time the technology has changed considerably—the blowpipe has been replaced by bellows and the construction of the furnace is different.

Some ancient metallic objects are presently being investigated by DSC and TMA measurements. For such studies a fragment of an original Osiris statuette, which is known to be manufactured from bronze, was used (Fig. 21b).

The chemical analysis of various ancient Egyptian bronzes (shown in Table 5) proved that the older metal alloys from the Old and Middle Kingdoms (2500–1300 B.C.) did not contain tin, whereas the bronzes from the New Kingdom and Late Period (1300 B.C.–300 A.D.) all contained tin

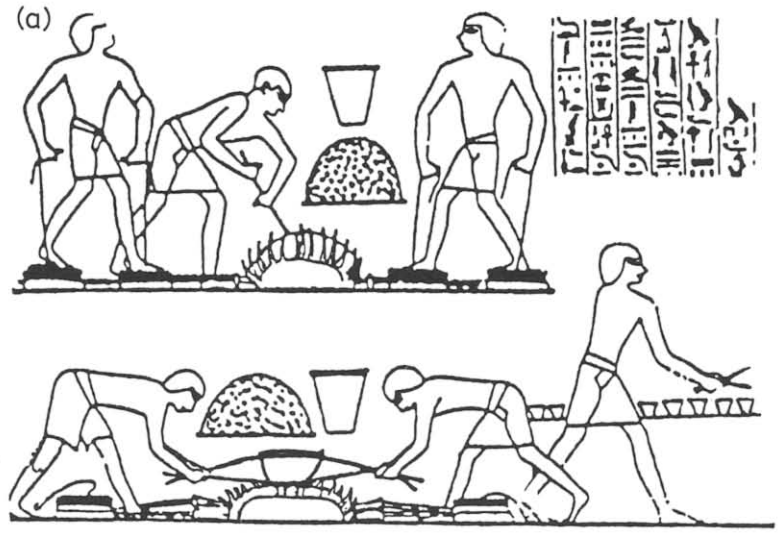

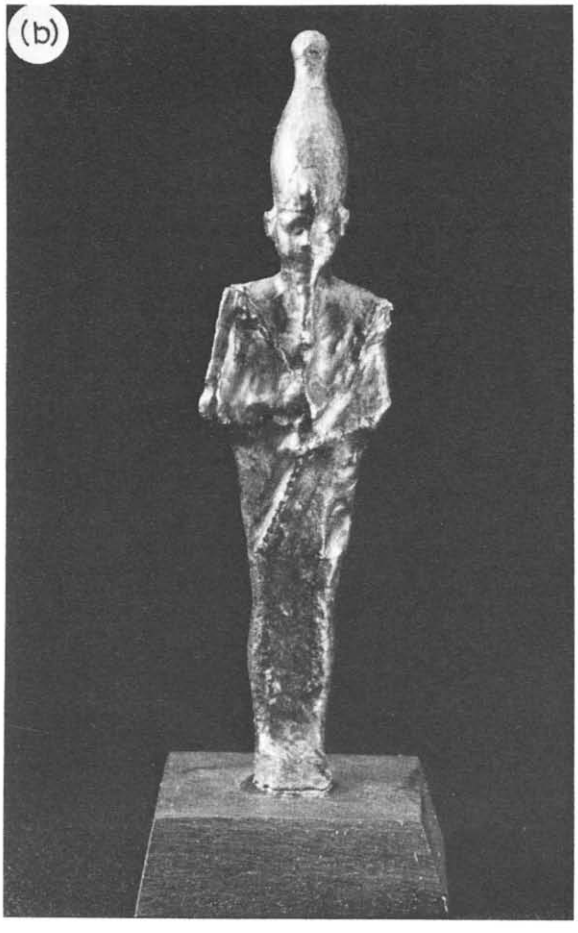

Fig. 21. (a) Melting of bronze in ancient Egypt (Tomb of Rehmire, Theben West, Egypt). (b) Bronze statuette of Osiris (Late period, 700 B.C.).

TABLE 5

Chemical analysis of ancient Egyptian bronzes [6]

	Cu	Sn	Pb	Zn	Fe	Ni	Ag	Sb	As
Old and Middle Kingdoms									
	99.09	–	0.15	–	0.02	0.01	0.04	0.02	0.67
	98.62	–	0.05	–	0.03	0.01	0.02	0.02	1.25
	97.66	–	0.07	–	0.20	0.01	0.02	–	2.04
	97.28	–	0.19	0.02	0.48	0.01	0.04	0.04	1.94
	97.01	–	0.24	0.02	0.45	0.01	0.04	0.04	2.19
New Kingdom and Late Period									
Osiris	96.83	1.12	0.85	0.01	0.91	0.02	0.07	0.04	0.15
Cat	95.02	4.22	0.14	–	0.35	0.01	0.02	0.02	0.22
Ptah	87.34	10.14	2.10	0.02	0.04	0.08	0.05	0.07	0.14
Anubis	84.71	14.12	0.72	0.01	0.11	0.12	0.04	0.01	0.16
Buto	83.02	6.80	9.72	–	0.08	0.08	0.04	0.19	0.07

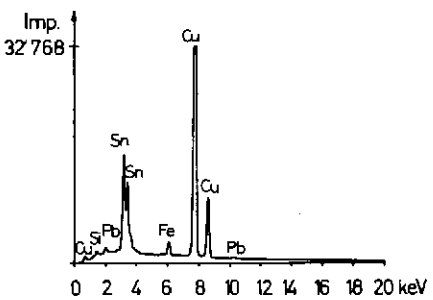

Fig. 22. EDAX of ancient Egyptian bronze.

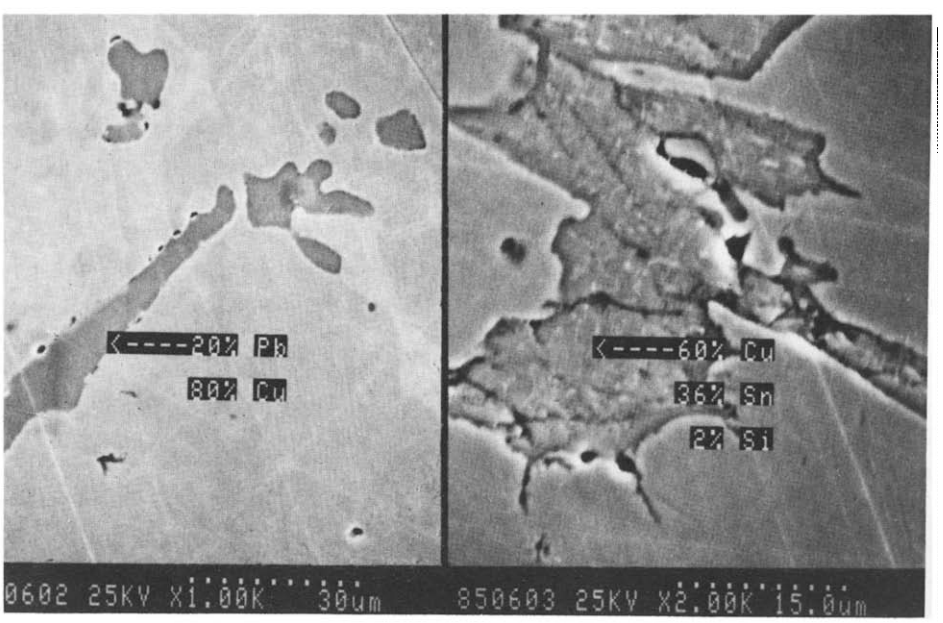

Fig. 23. BSE picture of ancient Egyptian bronze.

up to a concentration of about 15%. The sample used in the present investigation came from the beginning of the Late Period and contained, on average, 95% Cu, > 2% Sn, < 0.5% Pb and < 0.1% Fe, shown by the EDAX curve (Fig. 22). The homogeneity of this bronze, however, is very poor as may be seen from the back scattered electron micrographs (Fig. 23). There are both lead-rich and tin-rich segregations in the bronze matrix, due to poor homogenization and liquid immiscibility. This will also have an effect on the DSC and TMA curves. These curves show an interesting

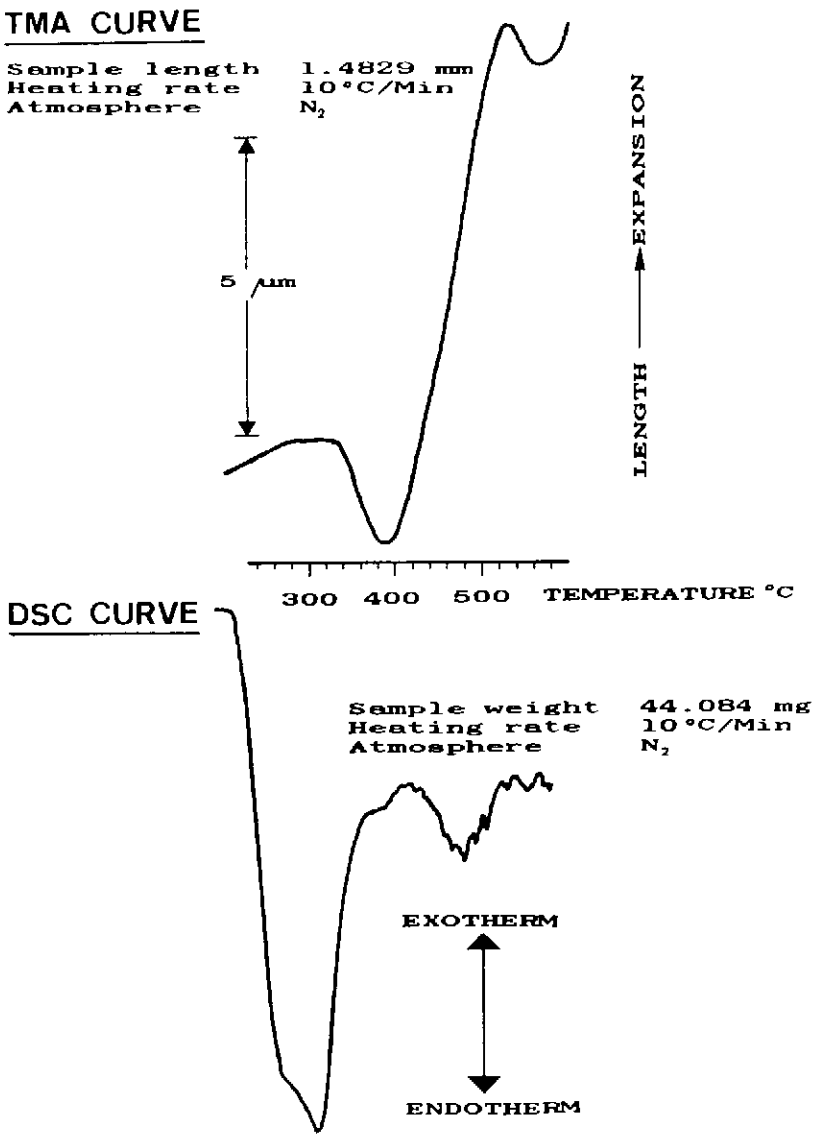

Fig. 24. DSC and TMA curves of ancient Egyptian bronze (Late Period, 700 B.C.).

similarity: the peak positions and drifts are probably related to phase transformations and partial melting (Fig. 24). Further investigations are necessary to correlate these effects with the phase diagram, as has been tried preliminarily.

CHINESE SILK [12]

The raising of silkworms and the making of silk have held an important place in Chinese cultural history for some five thousand years. Numerous accounts of the origins of silk are found in Chinese history and mythology. The real cradle of silk was the province of Shandong, where silk fabrics were first made at the beginning of the third millenium B.C.

In the spring of 1982 archaeologists began excavations at a tomb found at a brick and tile plant in Mashan, 21 km northwest of Jangling county, Hubei province. Preliminary estimates suggest that the tomb dates from the middle or late Warring States period (475–221 B.C.), some 300 years earlier than the Han tomb in Mawangdui, Hunan province. Though small in scale, the tomb preserved a wealth of wondrously fine silk fabrics which throw new light on modern archaeology.

The decorations of bronze vessels with motifs which belong to silk production at the time of the Shou dynasty (400 B.C.) are shown in Fig. 25:

Fig. 25. The collection of mulberry tree leaves, a silkworm and the hand weaving of silk as shown in decorations on ancient bronze vessels (Sou Dynasty).

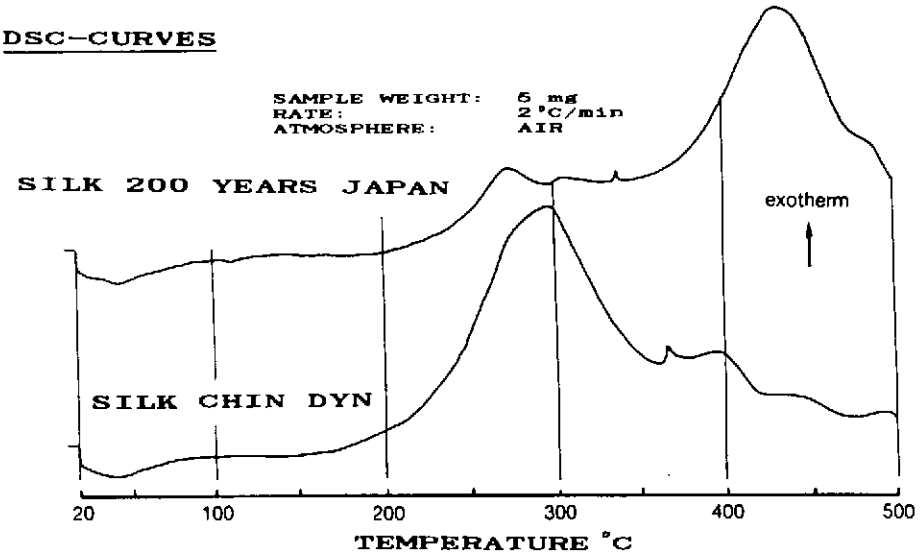

Fig. 26. DSC curves of ancient silk.

harvesting of mulberry tree leaves, a silkworm, and weaving of silk.

Figure 26 shows the results of DSC measurements on two ancient silk materials. The differences between these curves are probably due to different

TABLE 6

Writing of words in archaic and modern Chinese characters

ARCHAIC		TODAY
	Su: natural, simple, untreated	孫
	Sun: grandchild, posterity	裔
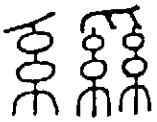	Yao: consequence as the chain of results	系

environmental effects which have changed the composition of the silk. Further measurements, however, are necessary for making a definite statement.

Further proof that silk was known even in very early times is supplied by the Chinese characters of the archaic period (approx. 16th to 17th Century B.C.). Any dictionary of Chinese etymology shows a whole series of characters derived from the silkworm, the cocoon, and the silk thread; for example the sign "su" is identical to the term for raw silk, the thread that is still covered by its fibrous layer, or the silk as it used to be harvested straight from the branches of the trees. This corresponds to concepts such as "natural", "simple" or "untreated". In the ideogram "sun", meaning "grandchild" or "posterity", the sequence of generations is represented by a

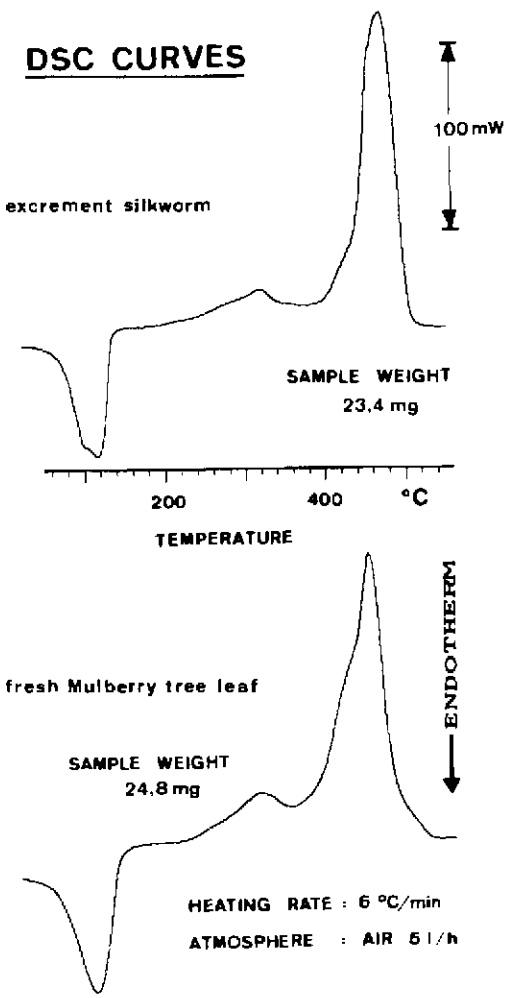

Fig. 27. DSC curves of mulberry tree leaf and of the silkworm excrement.

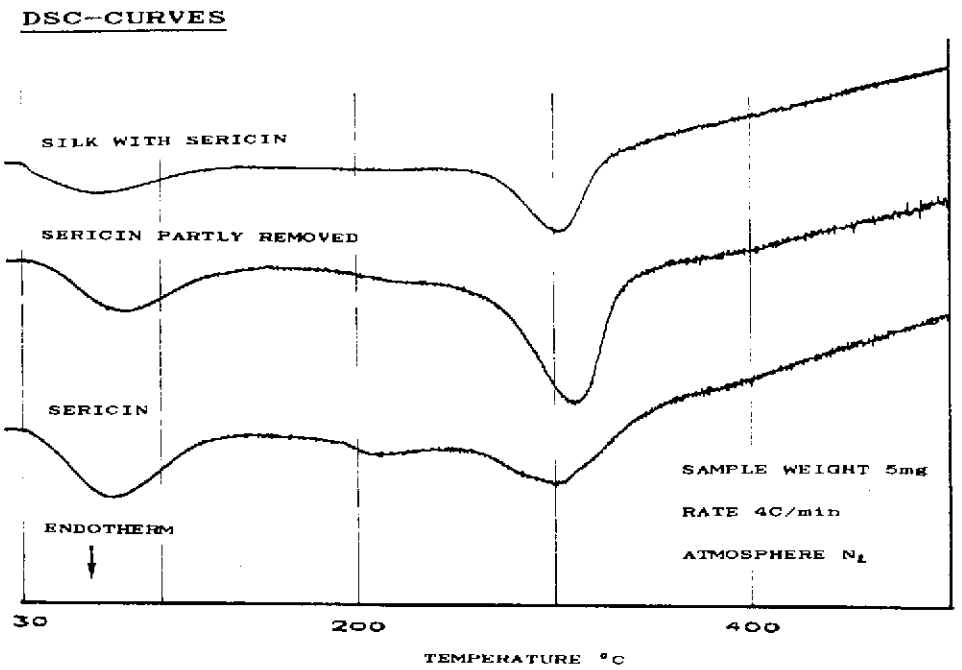

Fig. 28. DSC curves of raw silk, desericinized silk and sericin.

series of cocoons. The character for the word "yao" is similar in meaning, though with a subtle difference. It stands for the consequence as the chain of results deriving from a given cause. These few examples show how strongly familiar facts and objects of daily life have influenced Chinese characters and words (Table 6).

A comparison of our modern knowledge of the biological cycle of the silkworm, from egg to egg-laying moth through its many intervening metamorphoses, with the historical account given in the "Tiangong kaiwu" reveals no differences worthy of mention. At the beginning of June the small caterpillars hatch early one morning and creep out of the confined prison of their eggs that have lain till that time in a warm, moist environment. Some of them will not yet have reached maturity and will therefore wait until the next day or the day after to break through the shells of their eggs.

Figure 27 shows two DSC curves, the upper one from a fresh mulberry tree leaf and the lower one from the same leaf after it has been eaten by the silkworm and expelled as excrement. Differences are obvious from the shape of the dehydration peak and especially from the reduction of cellulose content, and from the change in the composition of the lignin.

The DSC curves in Fig. 28 are interesting for a comparison of raw silk (with sericin), of partially desericinized silk and of pure sericin. All these three samples lose water in the range 30–120°C, which results in an endothermic peak. According to the DSC curves, the H_2O content is higher

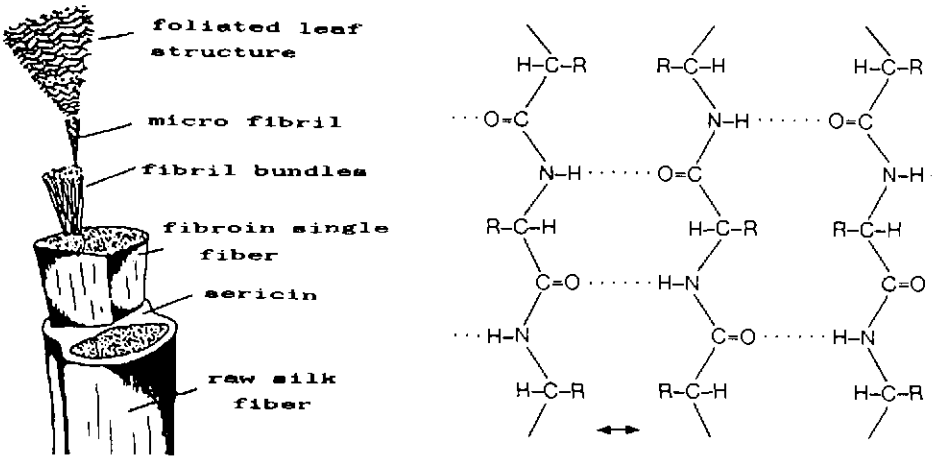

Fig. 29. Geometry and molecular structure of the silk fiber.

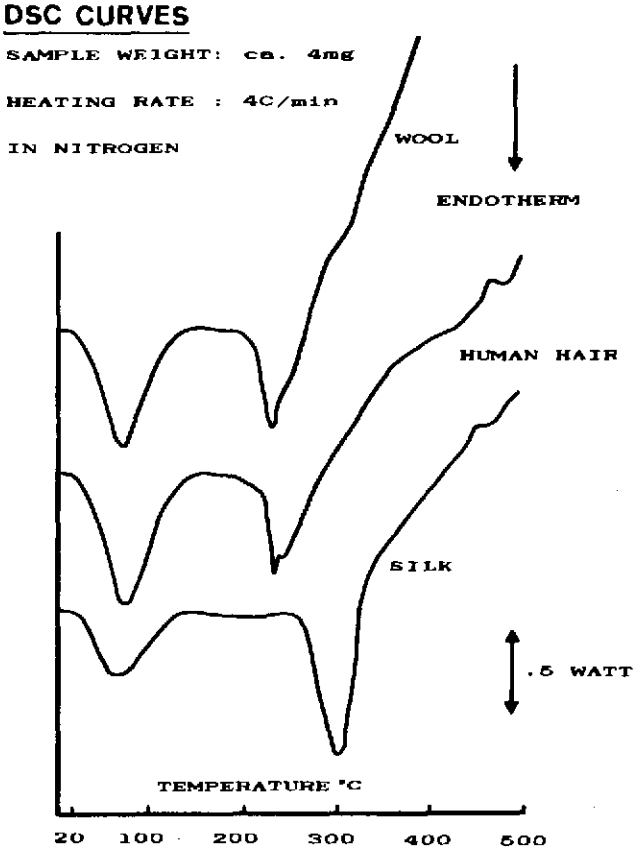

Fig. 30. DSC curves of wool, human hair and silk.

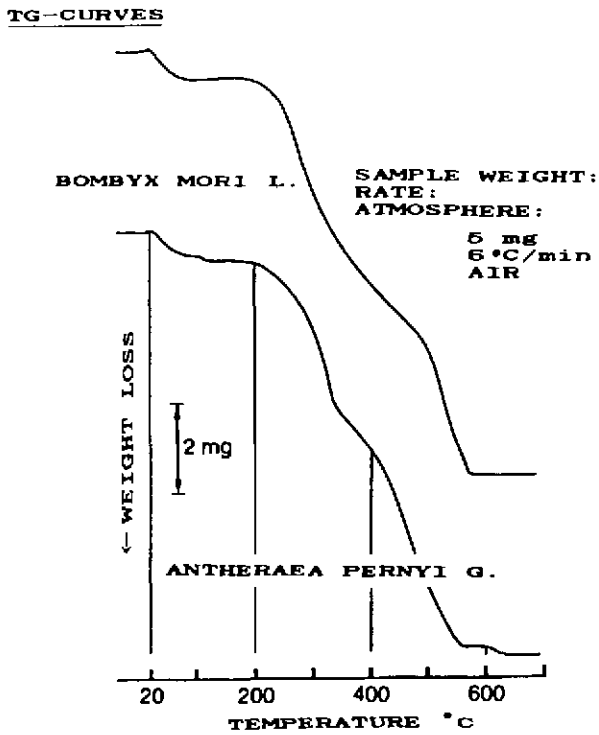

Fig. 31. TG curves of different raw silks.

in pure sericin than in silk. The decomposition of silk starts at about 260°C and is complete at 310°C. These temperatures are shifted to lower values for the less stable sericin. Following at higher temperatures, the degradation of the resulting carbon takes place.

The structure of a raw silk fiber may be seen in Fig. 29 in the form of a schematic drawing and as molecular, foliated leaf structure. The stretching direction of the fiber is marked with arrows and may also be seen by comparing the X-ray diagrams. As far as the thermal stability is concerned, both stretched and unstretched silk fiber behave identically.

DSC curves which compare wool, human hair, and silk prove that silk is thermally more stable (Fig. 30).

The double fiber of *Antherea pernŷ* is broader and less rounded as compared to the double fiber of *Bombyx mori*, the difference, however, is its covering with millions of whewellite crystals. This is characteristic of the spinnings of many Lepidopteres. Figures 31 and 32a show TG and DSC curves of these two different raw silks (*Antherea perny* and *Bombyx mori*). The TG curve shows the drying at 20–100°C, followed by dehydration of the smaller crystals at 20–100°C, by decomposition of the silk (up to 300°C) and by combustion of the generated carbon. These reaction steps are also

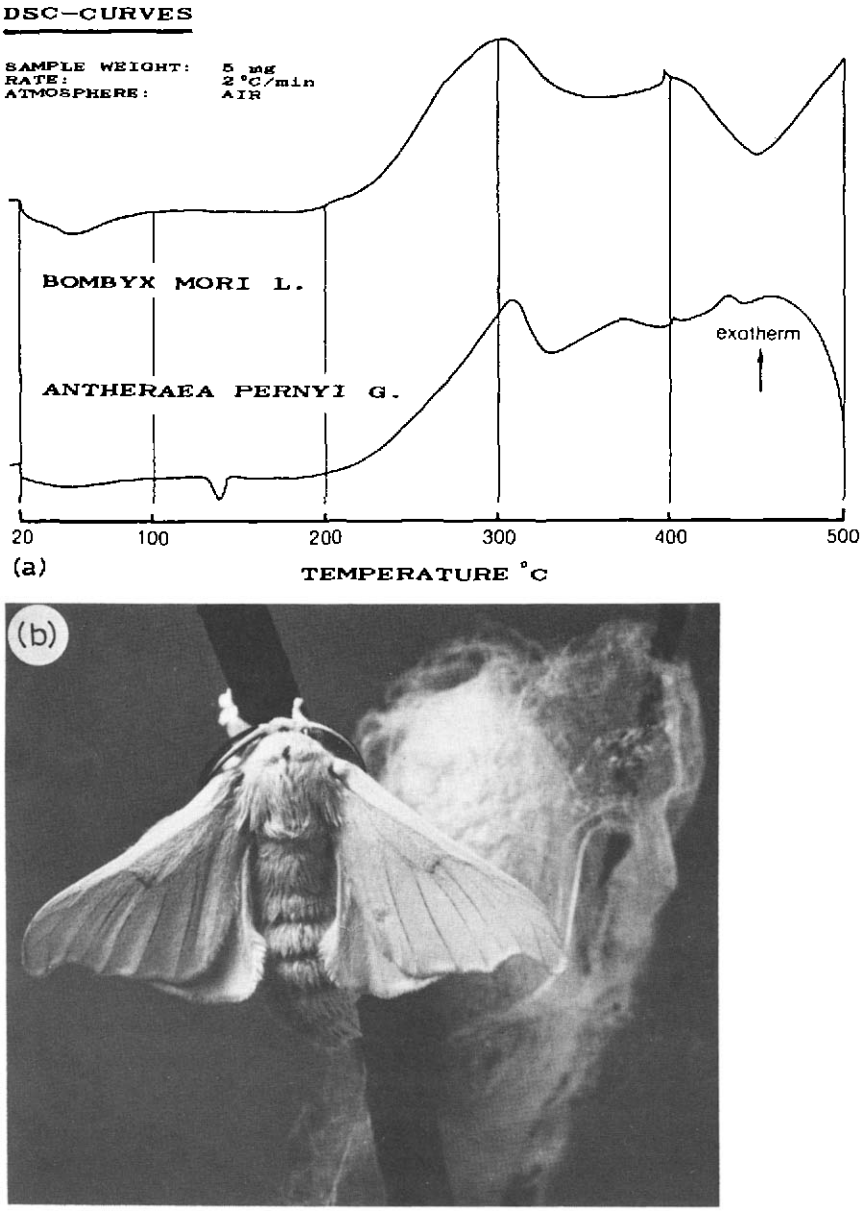

Fig. 32. (a) DSC curves of different raw silks. (b) The moth *Bombyx mori* with cocoon.

clearly demonstrated by the DSC curves in the form of endothermic and exothermic peaks at the corresponding temperatures. The silk fiber of the *Antherea perny* is thermally somewhat more stable and also stronger. All these measurements have been carried out in air. The difference to measurements in nitrogen atmosphere is that here no combustion of the silk takes

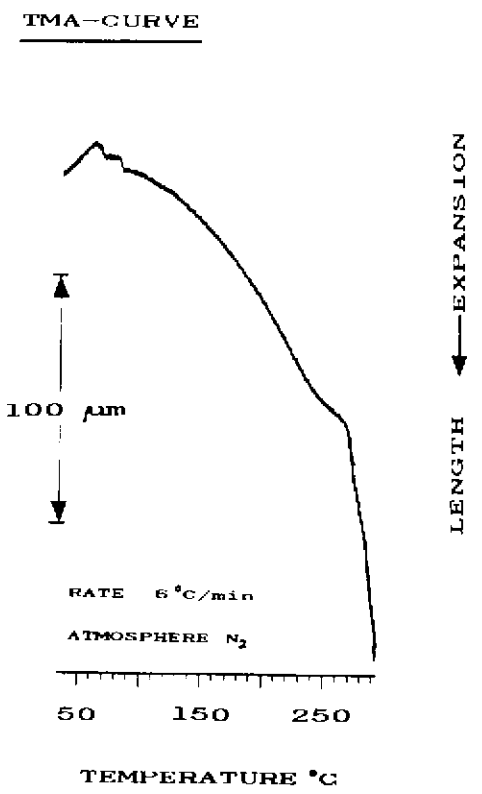

Fig. 33. TMA curve of raw silk fibers bundle (50 fibers).

place but only structural degradation. The moth *Bombyx mori* with cocoon is shown in Fig. 32b.

Figure 33 shows the application of a thermomechanical analysis (TMA) for determination of the expansion behavior of raw silk fibers. The silk thread (composed of 50 fibers) was clamped between a fixed position and the measuring sensor, and heated up uniformly. At the beginning there is a contraction followed by elastic deformation up to 260°C. Above this temperature plastic deformation takes place simultaneously with the degradation of the silk. The slight ripples in the curve at the beginning of the measurement are caused by sericin which has a different expansion behavior to fibricin.

CONCLUSIONS

Experimental results obtained on a variety of ancient objects prove that the combination of analytical pyrolysis and thermal analysis is a powerful tool in archaeometry.

Analysis of such precious objects is only possible because of the minute sample size required or because some of the methods are non-destructive.

It is particularly gratifying to show that such research can shed light on the past as well as pointing into the future.

On the old papyri fragments that have come down to us are these words of Hermes to Thoth: "It is difficult for reason to think of God, and for language to speak of Him. An immaterial entity cannot be described with material means. Whatever is eternal is very hard to unite with that which is subject to time's laws. The one passes, the other is forever. The one is a concept of the spirit, the other is a real thing. Anything that can be perceived with the eyes and the senses, such as visible bodies, can also be expressed in language. The incorporeal, invisible, non-material and formless cannot be grasped by our senses. I therefore see, O Thoth, that God is ineffable."

REFERENCES

1a S. Ratié, Hatschepsut, die Frau auf dem Thron der Pharaonen, F.A. Brockhaus, Wiesbaden, 1976.

1b A. Lucas, Ancient Egyptian Materials and Industries, 3rd edn., Arnold, London, 1959, p. 548.

2 G. Ebers, Papyrus Ebers, Verlag von Wilhelm Engelmann, Leipzig, 1875.

3 C. Basile, Conservation of Paintings and Graphic Arts, Lissabon Congress 1972, IIC, London, 1972, p. 901.

4 H.G. Wiedemann et al., in H. Chihara (Ed.), Thermal Analysis, Proc. 5th ICTA, Kyoto, 1977, Heyden, London, p. 373.

5 H.G. Wiedemann, Proc. 4th Int. Conf. on Surface and Colloid Chemistry, Israel, Jerusalem, 1981, p. 122.

6 J. Riederer, Kunstwerke Chemisch Betrachtet, Springer Verlag, Berlin, 1981.

7 K. Schmitt-Korte, Die Nabatäer, Spuren einer arabischen Kultur der Antike, Veröffentlichungen der Deutsch-Jordanischen Gesellschaft, e.V., Hannover, 1976.

8 G. Bayer and H.G. Wiedemann, Thermochim. Acta, 69 (1983) 167.

9 W.T. Chase, in R.H. Brill (Ed.), Egyptian Blue as a Pigment and Ceramic Material, MIT Press, Cambridge, MA, 1971, pp. 80–90.

10 W. Noll, Fortschr. Mineral., 57 (1971) 203.

11 G. Bayer and H.G. Wiedemann, Sandoz Bull., 40 (1976) 19; E. Iversen, Some Ancient Egyptian Paints and Pigments, Dan. Hist. Filol. Medd. 34, no. 4, 1955.

12 Ying-Hsing, T'ien-kung-k'ai wu (Chinese Technology in the Seventeenth Century), Pennsylvania State University Press, University Park, PA, 1966; K. Jörrissen, Über den thermischen Abbau von Keratinen, Dissertation, Aachen, Technische Hochschule, 1982.